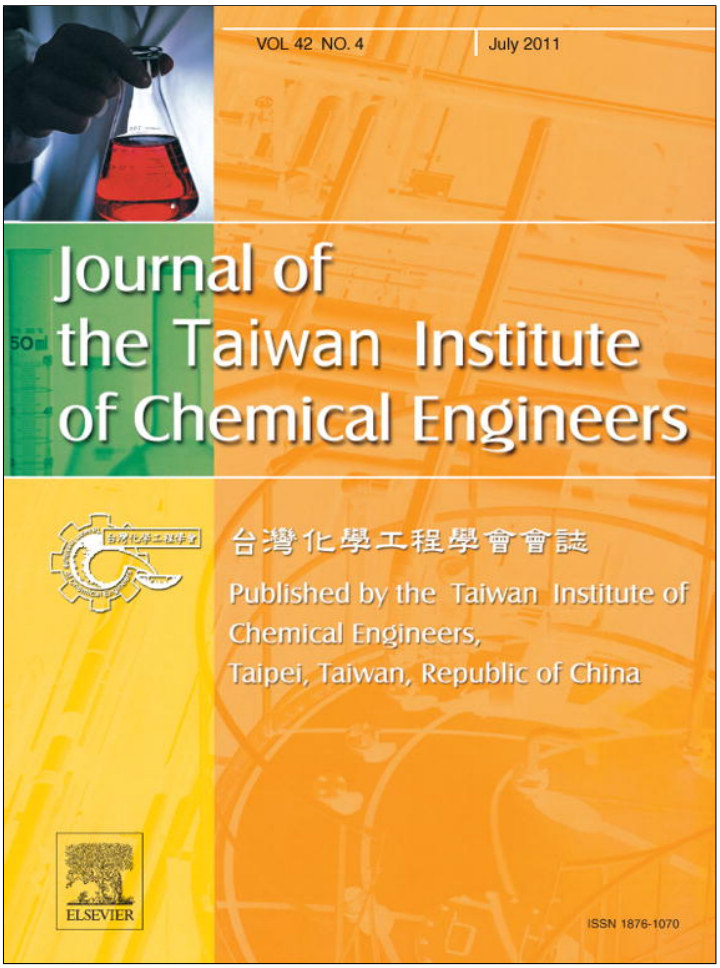

Journal of the Taiwan Institute of Chemical Engineers 42 (2011) 563–571

Contents lists available at ScienceDirect

Journal of the Taiwan Institute of Chemical Engineers

journal homepage: www.elsevier.com/locate/jtice

Drug design for hemagglutinin: Screening and molecular dynamics from traditional Chinese medicine database

Tung-Ti Chang [a,b], Mao-Feng Sun [a,c], Hsin-Yi Chen [d], Fuu-Jen Tsai [d,e], Calvin Yu-Chian Chen [a,d,f,*]

[a] Laboratory of Computational and Systems Biology, School of Chinese Medicine, China Medical University, Taichung 40402, Taiwan
[b] Department of Chinese Pediatrics, China Medical University Hospital, Taiwan
[c] Department of Acupuncture, China Medical University Hospital, Taiwan
[d] Department of Bioinformatics, Asia University, Taichung 41354, Taiwan
[e] Department of Medical Genetics, Pediatrics and Medical Research, China Medical University Hospital and College of Chinese Medicine, China Medical University, Taichung 40402, Taiwan
[f] Computational and Systems Biology, Massachusetts Institute of Technology, Cambridge, MA 02139, USA

ARTICLE INFO

Article history:
Received 5 September 2010
Received in revised form 28 October 2010
Accepted 11 November 2010
Available online 1 February 2011

Keywords:
H1N1
Influenza virus
Docking
Molecular dynamics
Traditional Chinese medicine (TCM) database

ABSTRACT

Since the outbreak of Swine flu, H1N1 virus had caused a global pandemic and resulted in more than 18,000 deaths over the world as dated on August 2010. Influenza virus surface glycoprotein, hemagglutinin, holds a critical role in mediating viral entry into host cell. Currently, there is no available hemagglutinin binding inhibitor, and already, influenza virus strains resistant to front-line antivirals have been discovered. Here, we report two rosmaricine derivatives might be potent leads which screening from the world largest traditional Chinese medicine database. The docking results shown the rosmaricine derivatives bind influenza hemagglutinin with high affinity based on binding energy. Both rosmaricine_5 and rosmaricine_16 have high binding energy and have hydrogen bonding with hemagglutinin sialic acid binding site residues, Glu83, Asp103 and Asn104. These interactions persist throughout the molecular dynamics simulation and keep the rosmaricine derivatives in the hemagglutinin sialic acid binding site. From the molecular dynamics results show that a potential hemagglutinin inhibitor should have a protonated amine for interacting with Asp103 and hydroxyl groups for interacting with Glu83 and Asn104. Overall, we suggest our two *de novo* compounds can become novel antivirals for treating influenza infection.

1. Introduction

Influenza viruses can be categorized into three subtypes, namely A, B and C, and among subtypes, influenza A virus is the most virulent and can infect humans, horses, pigs, mammals and birds (Webster *et al.*, 1992). In the past, several major pandemics had been caused by influenza A virus, including the 1918 Spanish flu (H1N1), the 1957 Asian flu (H2N2) and the 1968 Hong Kong flu (H3N2) (Nicholls, 2006). Most recently, the Swine flu (2009/H1N1 virus) had caused a global pandemic and resulted in more than 18,000 death over the world as dated on August 2010 (WHO, 2010).

The surface of influenza A virus contains two glycoproteins—hemagglutinin and neuraminidase. Hemagglutinin can be further divided into 15 different serotypes (H1–H15) (Suzuki and Nei, 2002). Of all serotypes, H1, H2 and H3 are the most commonly circulated. During the viral replication cycle, hemagglutinin (HA) has a critical role in the binding of virus to host surface sialic acid residues and fusion of the viral membrane to the host plasma membrane (Salomon and Webster, 2009). In terms of structure, HA is a trimer with each mature subunit composed of a HA1 chain responsible for sialic acid binding and a HA2 chain responsible for membrane fusion (Wharton *et al.*, 1995).

Currently, neuraminidase inhibitors, oseltamivir and zanamivir are still the front line anti-viral for treating influenza infection, but cases of oseltamivir resistant pandemic 2009 H1N1 viruses have been reported. M2 channel inhibitors, amantadine and rimantadine, that were effective in the past, are not recommended by WHO in 2009 H1N1 influenza pandemic due to drug resistance issues (Chen *et al.*, 2009b; Cheng *et al.*, 2009). To develop new anti-viral for treating influenza infection, we focused our attention on HA, specifically on subtype H1. Based on the before mentioned influenza viral replication strategy, a HA inhibitor could block viral entry into cells, thereby preventing generation of new viral progeny. In recent years, drug design using molecular simulations has gained importance and popularity. Molecular simulations have been conducted to investigate protein dynamics and protein–ligand interactions on

* Corresponding author. Current address: Computational and Systems Biology, Massachusetts Institute of Technology, Cambridge, MA 02139, USA.
Tel.: +1 617 353 7123.
E-mail addresses: ycc@mail.cmu.edu.tw, ycc929@MIT.EDU (C.-C. Chen).

1876-1070/$ – see front matter © 2011 Published by Elsevier B.V. on behalf of Taiwan Institute of Chemical Engineers.
doi:10.1016/j.jtice.2010.11.001

different topics (Bhargavi *et al.*, 2010; Cambria *et al.*, 2010; Cao and Wang, 2010; Chang *et al.*, 2010; Chen, 2010; da Cunha *et al.*, 2010; Huang *et al.*, 2010a,b; Kahlon *et al.*, 2010; Koshy *et al.*, 2010). Previously, we had conduced *in silico* studies on influenza hemagglutinin (Chen *et al.*, 2009a, 2010). As a continuation, we performed molecular dynamics simulation to further investigate ligand–H1 interaction. In the past, we have successfully conducted drug design by combining traditional Chinese medicine (TCM) and both ligand-based and structural-based drug design (Chen *et al.*, 2009a, 2010; Huang *et al.*, 2010a,b,c). We hope new success can be discovered by employing TCM on treating H1N1 infection.

2. Methods

2.1. Molecular modeling of H1N1 hemagglutinin

The hemagglutinin amino acid sequence of H1N1 was obtained from GenBank, source sequence accession CY061805. The protein template used for homology modeling was taken from Protein Data Bank, entry 1RVX (Gamblin *et al.*, 2004). A sequence alignment of the target and template, performed using the Clustal W program (Larkin *et al.*, 2007), showed high percent of sequence identity (80.4%) and similarity (89.5%) (Fig. 1) which supported using the template for homology modeling. The MODELLER program (Eswar *et al.*, 2006) implanted in Build Homology Models module of Discovery Studio 2.5 was used to build molecular model of hemagglutinin. The final model was evaluated by using Ramachandran graph and Verify-3D to ensure model quality.

2.2. Docking

A total of 20,000 natural products downloaded from the TCM Database@Taiwan (http://tcm.cmu.edu.tw/) were docked into the sialic acid binding site of hemagglutinin using LigandFit module of Discovery Studio 2.5 (Venkatachalam *et al.*, 2003). Prior to docking, CHARMm (Chemistry at Harvard Macromolecular Mechanics)

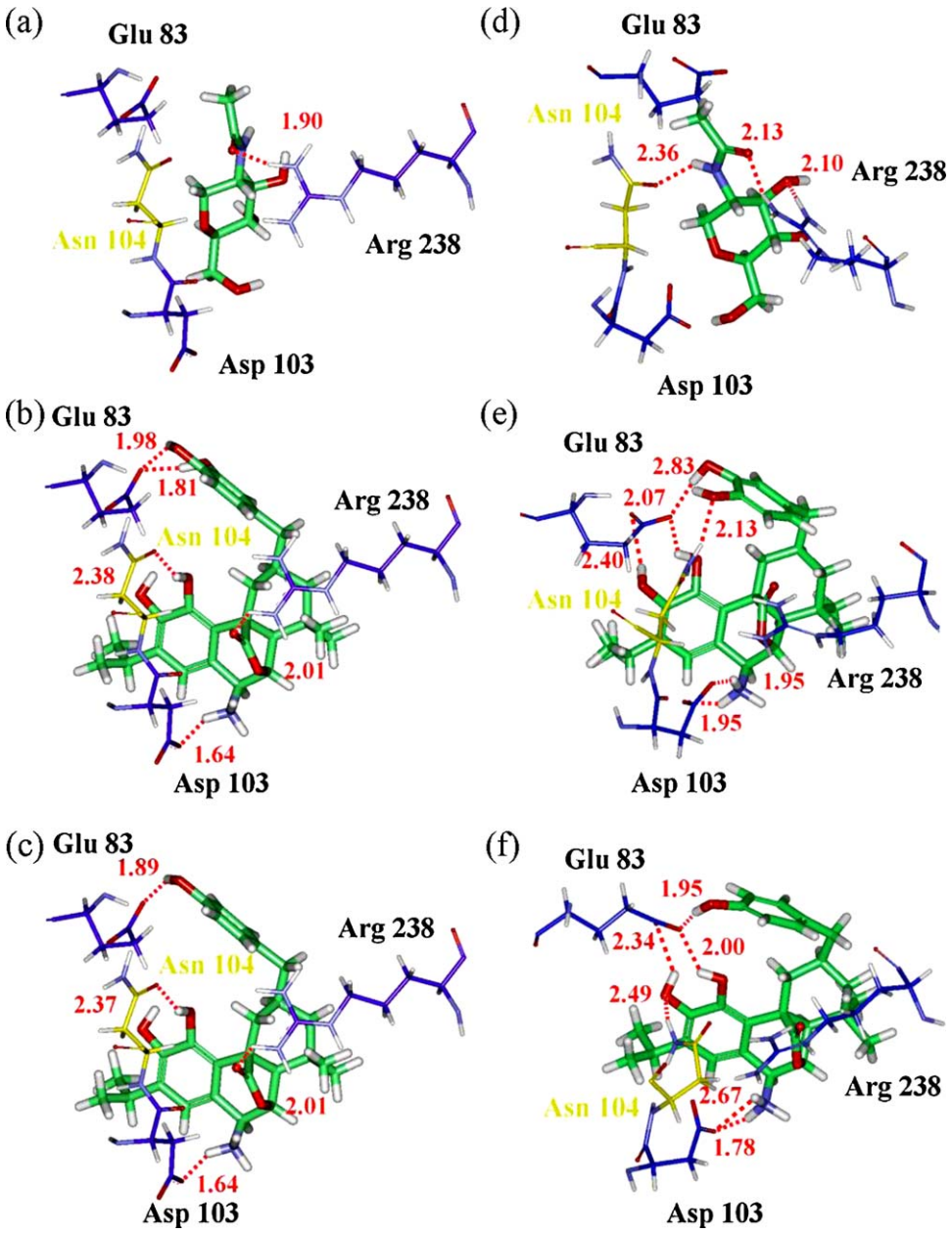

Fig. 1. Sequence alignment between the H1 crystal structure template 1RVX and the H1 target sequence. Sequence identity and similarity are 80.4% and 89.5%, respectively (Genbank accession ID: CY061805; protein ID: ADG08430).

force field was applied to the structure. The docking site was defined by the binding location of N-acetyl-D-glucosamine in the hemagglutinin template structure.

Ligand conformations generated in Monte Carlo simulation were placed into the binding site using a shape-based matching method. The protein was held rigid throughout docking while the ligands were allowed to orientate inside the binding pocket for sampling different binding poses. DREIDING force field was applied for calculating ligand–receptor interaction energies. Candidate ligand poses were energetically minimized using Smart Minimizer, which incorporates both Steepest Descent and Conjugate Gradient algorithm. Ligand poses were scored and ranked by binding energy. DockScore, potential mean force (PMF) and potential mean force 04 (PMF04) were also calculated for readers' interests. Compound N-acetyl-D-glucosamine (NAG) was used as control and was re-docked into the binding site for assessing binding affinity. The binding energy of NAG was used for filtering TCM compounds.

2.3. De novo design

After completing the docking screens, TCM compounds with binding energy higher than NAG were chosen for *de novo* design. The *De Novo* Evolution module of receptor–ligand interactions in Discovery Studio 2.5 was used for generating derivatives. In *De Novo* Evolution, the Ludi algorithm was employed to generate interaction sites within the ligand docking location and to identify fragments that form favorable interactions with the interaction sites. Fragments that best complement the interaction sites were fused or linked to the existing TCM scaffolds.

To screen out compounds that may not be orally active drug, the Lipinski's Rule of Five was applied to the TCM *de novo* products. Derivatives that have molecular weight greater than 500 Da or contain excess number of hydrogen bond donors or acceptors or exceed the octanol–water partition coefficient were excluded for further analysis. Derivatives that passed the screen were docked back to the binding site to evaluate binding affinity and receptor–ligand interactions.

2.4. Molecular dynamics simulation

Selected TCM candidates, in complex with hemagglutinin, were taken for molecular dynamics simulation. CHARMm force field was applied to the protein complexes prior to simulation. Each protein–ligand system was first energetically minimized with 500 steps of Steepest Descent and 500 steps of Conjugate Gradient method. After minimization, the system was heated from 50 K to 310 K in a time interval of 50 ps. Following, the equilibration step was conducted for 200 ps in 310 K. The final production run was conducted in NVT ensemble at 310 K for 20 ns. Each MD simulation was conducted with SHAKE algorithm that constraints bonding to hydrogen atoms. The time step was set for 0.001 ps. A snapshot was taken at every 2.5 ps. A total of 4000 snapshots were taken for a ligand–hemagglutinin complex.

The root mean square deviation (RMSD) of the protein and the ligand were computed for accessing protein stability. Hydrogen bond analysis was performed for analyzing key receptor–ligand interactions. The distance for hydrogen bond was set as 2.5 Å. Energy trajectory was also computed for investigating thermodynamic stability of the protein–ligand complex.

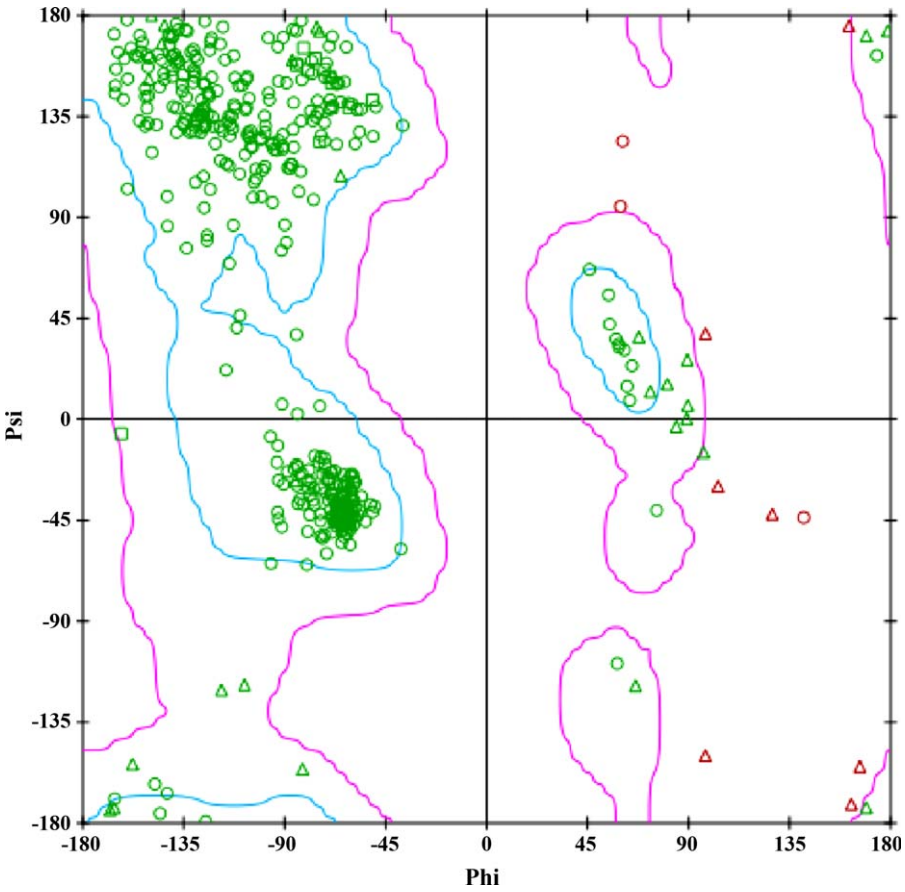

Fig. 2. Ramachandran graph, with 91.53% of residues in the favorable regions and 8.47% of residues in the disfavored or semi-allowed regions.

3. Results and discussions

The sequence identity and similarity between the target and the template sequence are 80.4% and 89.5%, respectively (Fig. 1). To validate the modeled H1 structure, Ramachandran plot (Ramachandran *et al.*, 1963) was used to examine the compatibility of dihedral angles of protein backbone atoms. The results show that 91.53% of residues are found in the favorable regions while only 8.47% of residues are in the disallowed or semi-allowed regions (Fig. 2). In addition to Ramanchandran plot, we also performed Verify-3D to evaluate protein fitness. Verify-3D checks the influenza hemagglutinin structure by evaluating the compatibility of the HA sequences with the protein 3D structure (Luthy *et al.*, 1992). For our result, all the key residues in the HA binding site (Arg238, Asn104 and Asn81) have Verify-3D scores greater than 1 (Fig. 3). These results further support the usage of the HA model.

3.1. Docking results

Results from docking and scoring of the TCM compounds and TCM derivatives are shown in Tables 1 and 2, respectively. The top *de novo* products, rosmaricine_5 and rosmaricine_16, are derivatives of rosmaricine, which could be isolated from leaves of rosemary (*Rosmarinus officinales*) (Calabrese *et al.*, 2000). Rosemary has hepatoprotective and antitumerogenic activity and is also an antioxidant (al-Sereiti *et al.*, 1999); furthermore, other rosmaricine derivatives have also been studied as potential antitumor agents (Boido *et al.*, 1994). Previously, natural compounds have been reported for antiviral anti-inflammatory and anti-oxidant effects (Chang *et al.*, 2009; Lai *et al.*, 2009); in addition, compounds isolated from *Ferula assafoetida* have been shown for antiviral activity (Lee *et al.*, 2009). Our study adds to the pool of natural compounds that have been shown to possess therapeutic potential.

The structures of the top two derivatives and the control are shown in Table 3. The docking poses of NAG, rosmaricine_5 and rosmaricine_16 are shown in Fig. 4(a)–and (c). Both rosmaricine_5 and rosmaricine_16 share addition of a hydroxyl substituted benzene ring and have very similar docking poses (Fig. 4(a) and (b)). The only difference is that rosmaricine_5 can establish two hydrogen bonds to Glu83 via the two added hydroxyl groups.

3.2. Molecular dynamics simulation

To examine the interactions between TCM compound and hemagglutinin, we selected the top two derivatives and the control for molecular dynamics simulations. The difference between docking poses and the snapshots taken at the end of molecular simulations are shown in Fig. 4(b), (d) and (f). As shown in Fig. 4(a) and (d), the control, NAG, has dramatic changes in binding conformation after the simulation run. The control

Table 1
The docking results of TCM compounds. The top 20 compounds of the database are shown here.

Name	BE	DS	PMF	PMF04
Camptothecin	−120.76	41.925	80.81	20.42
Catharanthine	−119.98	60.341	31.84	16.72
Magnoflorine	−117.94	46.071	57.63	30.84
Colchamine	−101.23	47.745	66.07	18.37
Heliotrine	−100.46	78.17	50.39	23.26
Rosmaricine	−100.44	79.093	71.28	24.89
Yohimbine	−98.33	74.02	48.18	29.04
Uncarine_A	−98.09	66.364	25.43	14.99
Peimisine	−97.98	79.552	69.12	15.76
Piperine	−92.84	44.495	46.23	7.04
Reserpine	−90.85	69.175	94.81	42.55
Mesembrine	−88.81	67.956	21.52	14.63
Physostigmine	−87.48	70.325	47.06	17.66
Evocarpine	−84.17	37.048	41.51	−0.04
Stephanine	−83.54	73.257	56.86	25.32
pingbeimine_C	−83.09	77.365	73.74	23.6
Cyclostachine_A	−81.18	46.609	72.71	16.68
Corydine	−79.43	83.07	58.75	28.79
Cinchonine	−76.92	76.956	34.42	19.04
Papaverine	−65.89	50.186	51.75	18.44
N-acetyl-D-glucosamine*	−52.81	49.69	59.89	29.43

BE: binding energy.
DS: dock score.
PMF: potential of mean force.
N-acetyl-D-glucosamine*: control.

Table 2
The docking results of top 5 derivatives.

Name	BE	DS	PMF	PMF04
Rosmaricine_5	−131.739	93.56	31.55	97.921
Rosmaricine_16	−120.762	88.38	27.92	96.528
Songbeisine_6	−108.648	75.46	16.9	72.679
Rhynchophylline_8	−98.931	61.73	30.08	85.757
Scopolamine_32	−98.397	61.05	24.68	90.164

BE: binding energy.
DS: dock score.
PMF: potential of mean force.
N-acetyl-D-glucosamine*: control.

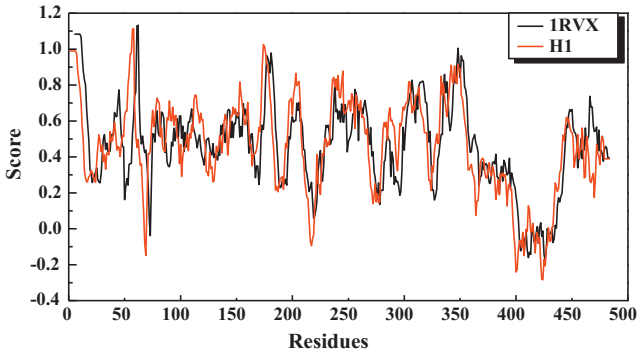

Fig. 3. Verify-3D result. Majority of protein residues have verify-3D scores greater than 1. Regions where scores have negative values have been investigated and these regions are not close to the binding site residues.

Table 3
The scaffold of control, original compounds, and derivatives.

Control	Original compounds
N-Acetyl-D-Glucosamine	Rosmaricine
Derivatives	
Rosmaricine_5	Rosmaricine_16

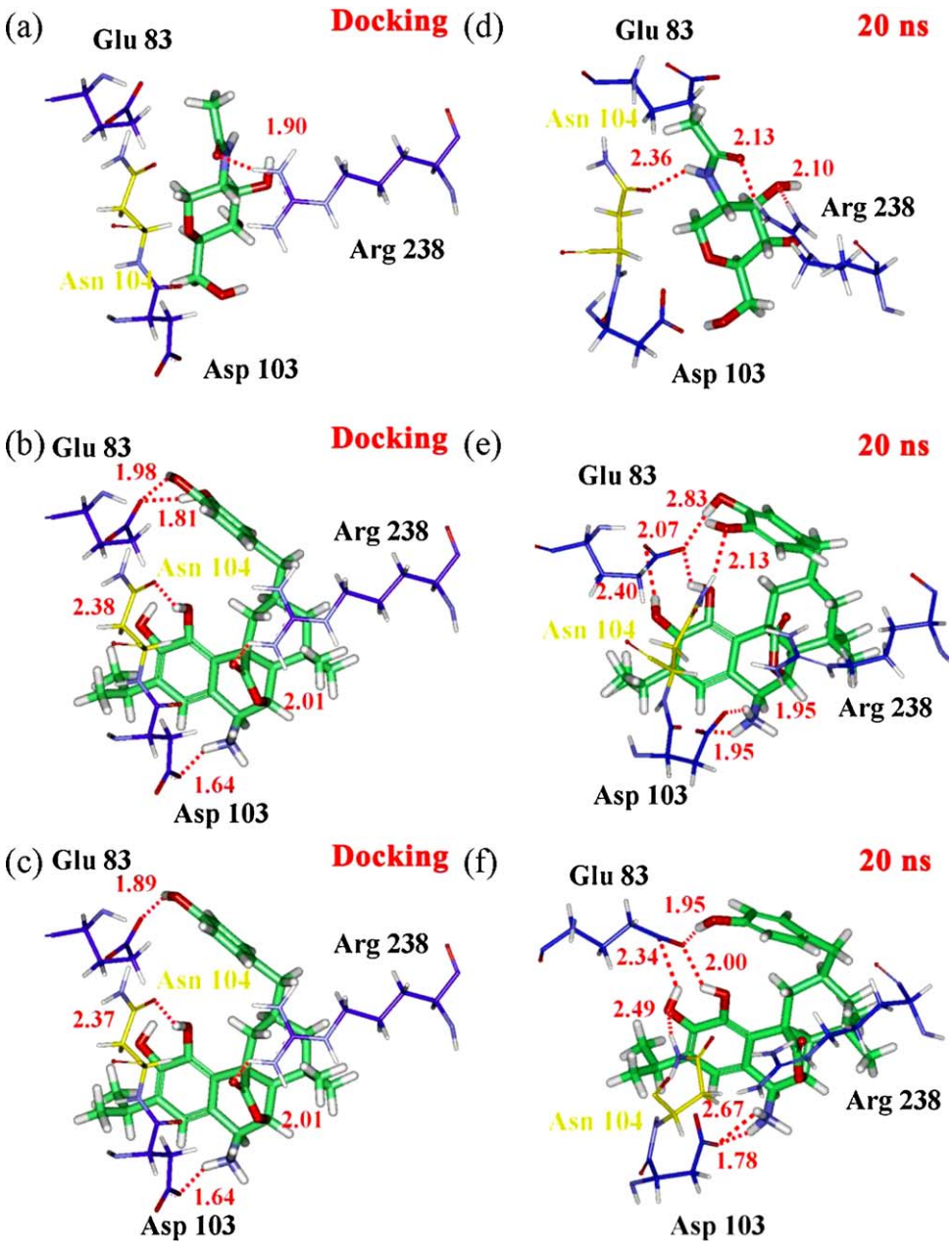

Fig. 4. The docking poses of the control and the top 3 derivatives in H1: (a) N-acetyl-D-glucosamine, (b) rosmaricine _5 and (c) rosmaricine_16. The snapshots taken at the end of molecular dynamics simulations are (d) N-acetyl-D-glucosamine, (e) rosmaricine _5 and (f) rosmaricine_16.

initially interacts with Arg238 via the amine functional group, but this hydrogen bonding is later changed to between the carbonyl group and Arg238. An additional hydrogen bonding is also formed between the hydroxyl group of the glucosamine and Arg238. At end of the simulation run, NAG interaction to Asn104 is also found.

For rosmaricine_5, the binding conformation is largely conserved, as observed from docking diagram and the snapshot from 20 ns. However, significant changes in binding site residues are found (Fig. 4(b) and (e)). More hydrogen bond interactions are observed between rosmaricine_5 and Glu83, with all interactions concentrate between ligand hydroxyl groups and Glu83 carboxylate side chain. Ligand hydrogen bond interactions to Asn104 and Asp103 are also observed; however the interacting locations are different for the docking pose and for the result obtained from molecular dynamics simulation (Fig. 4(b) and (e)). As for rosmaricine_16, the binding conformation after the simulation run is similar to that from rosmaricine_5 (Fig. 4(c) and (f)). Similar to rosmaricine_5, more hydrogen bonds are formed to Glu83. However, ligand interaction to Asp103 is less predominant due to changes in Asp103 substructure conformation.

To analyze the trajectories, we calculated whole molecule RMSD and ligand RMSD for the hemagglutinin–ligand complexes and the ligands. All ligand–protein complexes reach equilibrium during the simulation run as evidenced in whole molecule RMSD and ligand RMSD (Fig. 5). The energy trajectories show that both derivative-hemagglutinin complexes are much more stable than the control after the simulation run (Fig. 6).

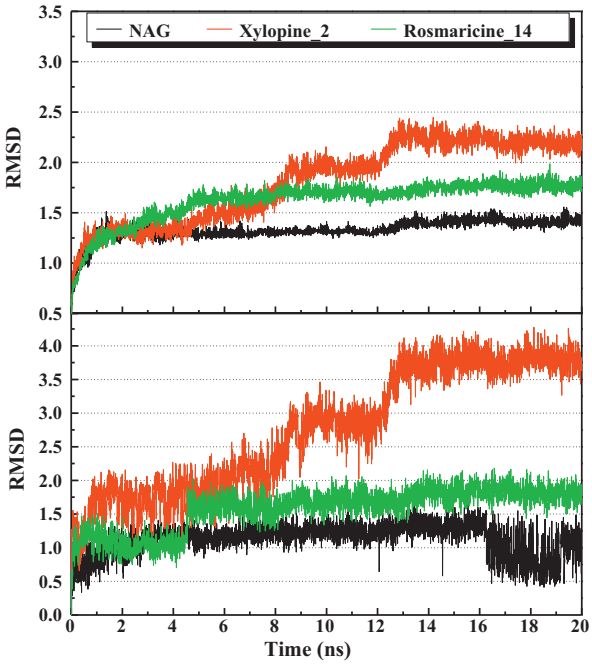

Fig. 5. The all atoms RMSD for N-acetyl-D-glucosamine (NAG) and top 2 candidates in H1 complexes during 20 ns simulation (top). The ligand RMSD is shown at bottom.

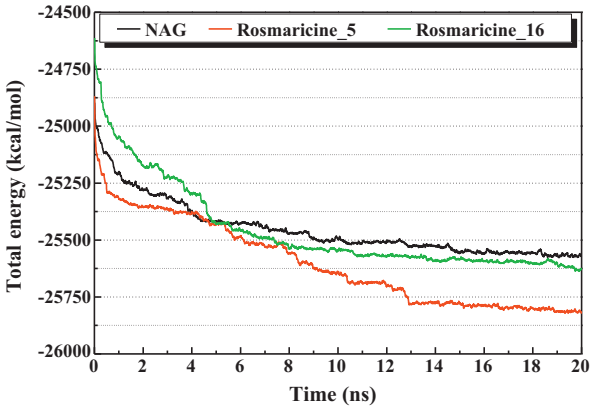

Fig. 6. The total energy of hemagglutinin in complex with N-acetyl-D-glucosamine (NAG) and top 2 candidates during 20 ns of simulation.

For all the hydrogen bonds observed from docking and molecular dynamics simulations, we summarized the hydrogen bond frequency (Tables 4–6) and computed the hydrogen bond distance trajectories (Figs. 7–9). For control, of all the interactions to Arg238, only two hydrogen bonds are continuously present and are under an average distance of 2.5 Å (Table 4). As for interaction to Asp103 and Asn104, all hydrogen bond distances fluctuate. Specifically, the interaction to Asp103 diminishes after 16 ns

Table 4
Hydrogen bond network formed between hemagglutinin and N-acetyl-D-glucosamine.

H-bond	Ligand atom	Amino acid	Max. distance	Min. distance	Average distance	H-bond occupancy
Distance1	O7	ARG238:HH12	2.83	1.59	1.91	99.68%
Distance2	O4	ARG238:HH21	4.43	2.13	3.63	3.68%
Distance3	O3	ARG238:HH22	2.89	1.66	2.18	95.40%
Distance4	O7	ARG238:HH22	3.54	2.03	2.75	7.53%
Distance5	H12	ASN104:OD1	3.70	1.99	2.81	16.13%
Distance6	H15	ASP103:OD1	3.78	2.05	2.64	28.60%
Distance7	H15	ASP103:OD2	4.10	1.78	2.42	71.03%

H-bond cutoff distance: 2.5 Å.

Table 5
Hydrogen bond network formed between hemagglutinin and rosmaricine_5.

H-bond	Ligand atom	Amino acid	Max. distance	Min. distance	Average distance	H-bond occupancy
H-bond_1	O1	ARG238:HE	5.82	2.41	3.94	0.05%
H-bond_2	O1	ARG238:HH21	5.16	1.64	2.90	43.03%
H-bond_3	O1	ARG238:HH22	5.10	2.37	3.67	0.13%
H-bond_4	O1	ASN104:HD22	4.70	2.31	3.88	0.05%
H-bond_5	O28	ASN104:HD22	4.31	2.46	3.40	0.03%
H-bond_6	O28	ASN104:HD21	3.07	1.78	2.28	80.65%
H-bond_7	O31	ASN104:HD21	3.78	1.89	2.72	26.00%
H-bond_8	O56	ASN104:HD22	3.44	1.77	2.46	57.15%
H-bond_9	H29	GLU83:OE2	2.60	1.73	1.96	99.98%
H-bond_10	H29	GLU83:OE1	4.17	2.12	3.45	1.75%
H-bond_11	H32	GLU83:OE1	3.31	1.92	2.69	18.55%
H-bond_12	H32	GLU83:OE2	3.85	1.76	2.45	60.55%
H-bond_13	H50	ASP103:OD1	3.71	1.60	2.46	62.23%
H-bond_14	H50	ASP103:OD2	4.39	1.79	3.11	23.40%
H-bond_15	H51	ASP103:OD1	3.73	1.60	2.54	58.63%
H-bond_16	H51	ASP103:OD2	4.35	1.80	3.01	33.50%
H-bond_17	H52	ASP103:OD1	3.72	1.58	2.36	72.60%
H-bond_18	H52	ASP103:OD2	4.24	1.70	2.91	37.68%
H-bond_19	H55	GLU83:OE2	4.74	1.81	3.34	12.55%
H-bond_20	H68	GLU83:OE2	2.46	1.66	1.93	100.00%

H-bond cutoff distance: 2.5 Å.

Table 6
Hydrogen bond network formed between hemagglutinin and rosmaricine_16.

H-bond	Ligand atom	Amino acid	Max. distance	Min. distance	Average distance	H-bond occupancy
H-bond_1	O31	ASN104:HD22	3.29	1.91	2.46	59.03%
H-bond_2	H29	GLU83:OE2	2.46	1.72	1.99	100.00%
H-bond_3	H32	GLU83:OE2	2.41	1.68	1.96	100.00%
H-bond_4	H50	ASP103:OD1	3.46	1.59	2.35	68.63%
H-bond_5	H51	ASP103:OD1	3.55	1.56	2.44	59.78%
H-bond_6	H52	ASP103:OD1	3.50	1.59	2.39	66.43%
H-bond_7	H55	GLU83:OE2	2.56	1.71	1.97	99.90%

H-bond cutoff distance: 2.5 Å.

(Fig. 7 and supplementary video). For rosmaricine_5, the initial interaction to Arg238 is unstable, and the separating distance could be as large as 5.82 Å (Table 5). The most stable interaction is the hydrogen bonding between rosmaricine_5 and Glu83 and Asn104 in which most hydrogen bonding persist throughout the simulation. The distance between Asn104 to rosmaricine_5 was relatively unchanged throughout the simulation (Fig. 8). This is in contrast to interaction to Asp103 in which the distance appears to be periodically changing over simulation time. For rosmaricine_16, the ligand has very stable interaction to Glu83 and Asn104 (Table 6 and Fig. 9). However, the interaction to Asp103 is less stable and has large fluctuations in bonding distance (Fig. 9).

After careful analysis of the docking and molecular dynamics simulation results, we observed that the ligands interact predominantly to Glu83, Asp103 and Asn104. The main interacting functional groups found on the ligands are (1) the protonated primary amine, (2) the added hydroxyl groups and (3) the hydroxyl groups found on the main scaffold (Fig. 10). The protonated amine group interacts with Asp103 in the form of salt bridge interaction while the other hydroxyl groups act as hydrogen bond donors and bind to Glu83 and Asn104. We conclude that these functional domains found on rosmaricine derivatives are the key structures responsible for inhibitory activity. In addition, to inhibit influenza hemagglutinin, stable interactions to Glu83 and Asn104 appear to us as the basic requirements.

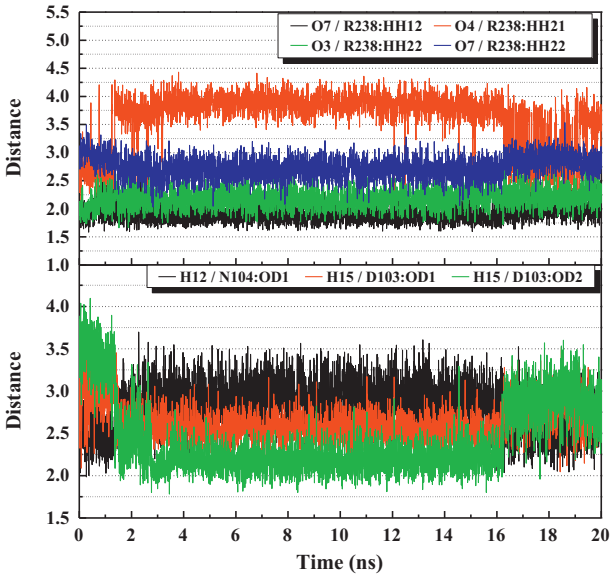

Fig. 7. Time dependent hydrogen bond distance between N-acetyl-D-glucosamine and hemagglutinin residues: Arg 238, Asn 103 and Asp 104.

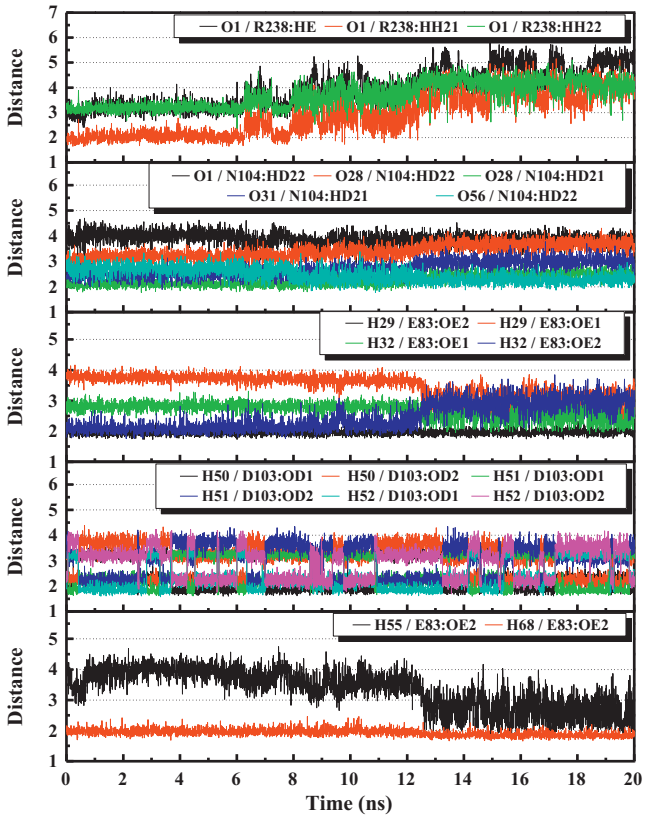

Fig. 8. Time dependent hydrogen bond distance between rosmaricine_5 and hemagglutinin residues.

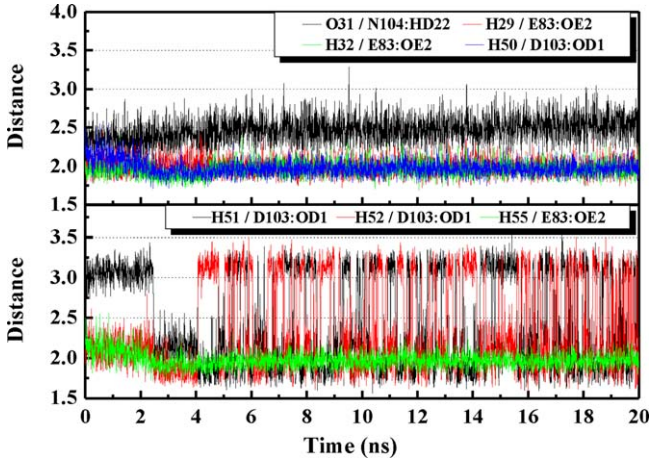

Fig. 9. Time dependent hydrogen bond distance between rosmaricine_16 and hemagglutinin residues.

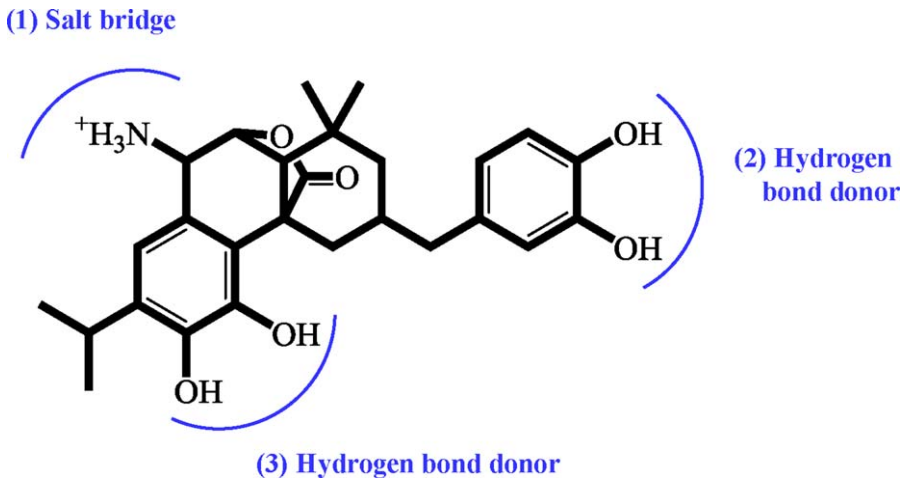

Fig. 10. The three features for designing drugs targeting H1.

4. Conclusion

The wide spread of influenza A (H1N1) virus had overwhelmed the health authorities worldwide with the number of infected cases. Influenza viral surface glycoprotein, hemagglutinin, has an important role in viral replication cycle and therefore, is a very potential therapeutic target. Here, we show two rosmaricine derivatives, rosmaricine_5 and rosmaricine_16, as potent inhibitors for blocking hemagglutinin binding to sialic acid residues. Both derivatives share similar binding poses and establish continuous hydrogen bonding to key binding site residues, Asn104 and Glu83. Structural analysis of rosmaricine derivatives suggests a hemagglutinin inhibitor should contain a protonated amine group for interacting with Asp103 and two hydroxyl groups substituted domains for interacting with Glu83 and Asn104. We anticipate our two derivatives can be further developed into next generation of antivirals for treating influenza infection.

Acknowledgements

The research was supported by grants from the National Science Council of Taiwan (NSC 99-2221-E-039-013), China Medical University (CMU98-TCM, CMU99-S-02) and Asia University (CMU98-ASIA-09). This study is also supported in part by Taiwan Department of Health Clinical Trial and Research Center of Excellence (DOH99-TD-B-111-004) and Taiwan Department of Health Cancer Research Center of Excellence (DOH99-TD-C-111-005). We are grateful to the National Center of High-performance Computing for computer time and facilities.

Appendix A. Supplementary data

Supplementary data associated with this article can be found, in the online version, at doi:10.1016/j.jtice.2010.11.001.

References

al-Sereiti, M. R., K. M. Abu-Amer, and P. Sen, "Pharmacology of Rosemary (Rosmarinus Officinalis Linn.) and Its Therapeutic Potentials," *Indian J. Exp. Biol.*, **37**, 124 (1999).

Bhargavi, K., P. K. Chaitanya, D. Ramasree, M. Vasavi, D. K. Murthy, and V. Uma, "Homology Modeling and Docking Studies of Human Bcl-2l10 Protein," *J. Biomol. Struct. Dyn.*, **28**, 379 (2010).

Boido, A., F. Savelli, and F. Sparatore, "Rosmaricine Derivatives as Potential Antitumoral Agents," *Farmaco*, **49**, 111 (1994).

Calabrese, V., G. Scapagnini, C. Catalano, F. Dinotta, D. Geraci, and P. Morganti, "Biochemical Studies of a Natural Antioxidant Isolated from Rosemary and Its Application in Cosmetic Dermatology," *Int. J. Tissue React.: Exp. Clin. Aspects*, **22**, 5 (2000).

Cambria, M. T., D. Di Marino, M. Falconi, S. Garavaglia, and A. Cambria, "Docking Simulation and Competitive Experiments Validate the Interaction between the 2,5-Xylidine Inhibitor and Rigidoporus Lignosus Laccase," *J. Biomol. Struct. Dyn.*, **27**, 501 (2010).

Cao, Z. X. and J. H. Wang, "A Comparative Study of Two Different Force Fields on Structural and Thermodynamics Character of H1 Peptide Via Molecular Dynamics Simulations," *J. Biomol. Struct. Dyn.*, **27**, 651 (2010).

Chang, T. T., H. J. Huang, K. J. Lee, H. W. Yu, H. Y. Chen, F. J. Tsai, M. F. Sun, and C. Y. C. Chen, "Key Features for Designing Phosphodiesterase-5 Inhibitors," *J. Biomol. Struct. Dyn.*, **28**, 309 (2010).

Chen, C. Y. C., "Virtual Screening and Drug Design for Pde-5 Receptor from Traditional Chinese Medicine Database," *J. Biomol. Struct. Dyn.*, **27**, 627 (2010).

Chen, C. Y., Y. H. Chang, D. T. Bau, H. J. Huang, F. J. Tsai, C. H. Tsai, and C. Y. C. Chen, "Ligand-Based Dual Target Drug Design for H1N1: Swine Flu—a Preliminary First Study," *J. Biomol. Struct. Dyn.*, **27**, 171 (2009a).

Chen, H., C. L. Cheung, H. Tai, P. Zhao, J. F. Chan, V. C. Cheng, K. H. Chan, and K. Y. Yuen, "Oseltamivir-Resistant Influenza A Pandemic (H1N1) 2009 Virus, Hong Kong, China," *Emerg. Infect. Dis.*, **15**, 1970 (2009b).

Chen, C. Y., H. J. Huang, F. J. Tsai, and C. Y. C. Chen, "Drug Design for Influenza A Virus Subtype H1N1," *J. Taiwan Inst. Chem. Engrs.*, **41**, 8 (2010).

Cheng, P. K., T. W. Leung, E. C. Ho, P. C. Leung, A. Y. Ng, M. Y. Lai, and W. W. Lim, "Oseltamivir- and Amantadine-Resistant Influenza Viruses a (H1N1)," *Emerg. Infect. Dis.*, **15**, 966 (2009).

da Cunha, E. F. F., E. F. Barbosa, A. A. Oliveira, and T. C. Ramalho, "Molecular Modeling of Mycobacterium Tuberculosis DNA Gyrase and Its Molecular Docking Study with Gatifloxacin Inhibitors," *J. Biomol. Struct. Dyn.*, **27**, 619 (2010).

Eswar, N., B. Webb, M. A. Marti-Renom, M. S. Madhusudhan, D. Eramian, M. Y. Shen, U. Pieper, and A. Sali, "Comparative Protein Structure Modeling Using Modeller," *Curr. Protoc. Bioinform.*, **Chapter 5**, 6 Unit 5.

Gamblin, S. J., L. F. Haire, R. J. Russell, D. J. Stevens, B. Xiao, Y. Ha, N. Vasisht, D. A. Steinhauer, R. S. Daniels, A. Elliot, D. C. Wiley, and J. J. Skehel, "The Structure and Receptor Binding Properties of the 1918 Influenza Hemagglutinin," *Science*, **303**, 1838 (2004).

Huang, H. J., K. J. Lee, H. W. Yu, C. Y. Chen, C. H. Hsu, H. Y. Chen, F. J. Tsai, and C. Y. C. Chen, "Structure-Based and Ligand-Based Drug Design for Her 2 Receptor," *J. Biomol. Struct. Dyn.*, **28**, 23 (2010a).

Huang, H. J., K. J. Lee, H. W. Yu, H. Y. Chen, F. J. Tsai, and C. Y. C. Chen, "A Novel Strategy for Designing the Selective Ppar Agonist by The "Sum of Activity" Model," *J. Biomol. Struct. Dyn.*, **28**, 187 (2010b).

Kahlon, A. K., S. Roy, and A. Sharma, "Molecular Docking Studies to Map the Binding Site of Squalene Synthase Inhibitors on Dehydrosqualene Synthase of Staphylococcus Aureus," *J. Biomol. Struct. Dyn.*, **28**, 201 (2010).

Koshy, C., M. Parthiban, and R. Sowdhamini, "100 Ns Molecular Dynamics Simulations to Study Intramolecular Conformational Changes in Bax," *J. Biomol. Struct. Dyn.*, **28**, 71 (2010).

Larkin, M. A., G. Blackshields, N. P. Brown, R. Chenna, P. A. McGettigan, H. McWilliam, F. Valentin, I. M. Wallace, A. Wilm, R. Lopez, J. D. Thompson, T. J. Gibson, and D. G. Higgins, "Clustal W and Clustal X Version 2.0," *Bioinformatics*, **23**, 2947 (2007).

Luthy, R., J. U. Bowie, and D. Eisenberg, "Assessment of Protein Models with Three-Dimensional Profiles," *Nature*, **356**, 83 (1992).

Nicholls, H., "Pandemic Influenza: The Inside Story," *PLoS Biol.*, **4**, 156 (2006).

Ramachandran, G. N., C. Ramakrishnan, and V. Sasisekharan, "Stereochemistry of Polypeptide Chain Configurations," *J. Mol. Biol.*, **7**, 95 (1963).

Salomon, R. and R. G. Webster, "The Influenza Virus Enigma," *Cell*, **136**, 402 (2009).
Suzuki, Y. and M. Nei, "Origin and Evolution of Influenza Virus Hemagglutinin Genes," *Mol. Biol. Evol.*, **19**, 501 (2002).
Venkatachalam, C. M., X. Jiang, T. Oldfield, and M. Waldman, "Ligandfit: A Novel Method for the Shape-Directed Rapid Docking of Ligands to Protein Active Sites," *J. Mol. Graph. Model.*, **21**, 289 (2003).
Webster, R. G., W. J. Bean, O. T. Gorman, T. M. Chambers, and Y. Kawaoka, "Evolution and Ecology of Influenza A Viruses," *Microbiol. Rev.*, **56**, 152 (1992).
Wharton, S. A., L. J. Calder, R. W. Ruigrok, J. J. Skehel, D. A. Steinhauer, and D. C. Wiley, "Electron Microscopy of Antibody Complexes of Influenza Virus Haemagglutinin in the Fusion Ph Conformation," *EMBO J.*, **14**, 240 (1995).
WHO. *Pandemic (H1N1) 2009—Update 112, http://www.who.int/csr/don/2010_08_06/en/.*